

# Towards deterministic optical quantum computation with coherently driven atomic ensembles

David Petrosyan\*

*Institute of Electronic Structure & Laser, FORTH, Heraklion 71110, Crete, Greece*

(Dated: March 19, 2018)

Scalable and efficient quantum computation with photonic qubits requires (i) deterministic sources of single-photons, (ii) giant nonlinearities capable of entangling pairs of photons, and (iii) reliable single-photon detectors. In addition, an optical quantum computer would need a robust reversible photon storage device. Here we discuss several related techniques, based on the coherent manipulation of atomic ensembles in the regime of electromagnetically induced transparency, that are capable of implementing all of the above prerequisites for deterministic optical quantum computation with single photons.

PACS numbers: 03.67.Lx, 42.50.Gy

## I. INTRODUCTION

The field of quantum information, which extends and generalizes the classical information theory, is currently attracting enormous interest in view of its fundamental nature and its potentially revolutionary applications to computation and secure communication [1, 2]. Among the various schemes for physical implementation of quantum computation [3, 4, 5, 6, 7, 8], those based on photons [7, 8] have the advantage of using very robust and versatile carriers of quantum information. However, the absence of practical single-photon sources and the weakness of optical nonlinearities in conventional media [9] are the major obstacles for the realization of efficient all-optical quantum computation. To circumvent these difficulties, it has been proposed to use linear optical elements, such as beam-splitters and phase-shifters, in conjunction with parametric down-converters and single-photon detectors, for achieving probabilistic quantum logic with photons conditioned on the successful outcome of a measurement performed on auxiliary photons [8]. Yet, an efficient and scalable device for quantum information processing with photons would ideally require deterministic sources of single photons, strong nonlinear photon-photon interaction and reliable single-photon detectors. In addition, a versatile optical quantum computer would need a robust reversible memory device.

In this paper we discuss several related techniques which can be used to implement all of the above prerequisites for deterministic optical quantum computation. The schemes discussed below are based on the coherent manipulation of atomic ensembles in the regime of electromagnetically induced transparency (EIT) [10, 11, 12, 13], which is a quantum interference effect that results in a dramatic reduction of the group velocity of weak propagating field accompanied by vanishing absorption [14]. As the quantum interference is usually very sensitive to

the system parameters, various schemes exhibiting EIT have recently received considerable attention due to their potential for greatly enhancing nonlinear optical effects. Some of the most representative examples include slow-light enhancement of acousto-optical interactions in doped fibers [15], trapping light in optically dense atomic and doped solid-state media by coherently converting photonic excitation into spin excitation [16, 17, 18] or by creating photonic band gap via periodic modulation of the EIT resonance [19], and nonlinear photon-photon coupling using N-shaped configuration of atomic levels [20, 21, 22, 23].

Below, we will focus on the optical implementation of quantum computation with qubit basis states represented by two orthogonal polarization states of single photons, as opposed to an alternative approach, wherein nearly-orthogonal weak coherent states of optical fields are used [24, 25]. The chief motivation for this is that single-photon pulses provide a natural choice for qubits employed in quantum computation and quantum communication protocols [1, 2], and facilitate the convenience and intuitiveness in the description of their dynamics in quantum information processing networks.

In section II we outline the envisioned setup of an optical quantum computer and discuss the physical implementations of the required single- and two-qubit logic operations. Section III gives a concise introduction of the EIT in optically dense atomic media, which is necessary for understanding the principles of operation of photonic memory device of section IV, deterministic single photon sources discussed in section V, giant cross-phase modulation of section VI, and reliable single-photon detection presented in section VII. The conclusions are summarized in section VIII.

## II. OPTICAL QUANTUM COMPUTER

Quantum computer is an envisaged physical device for processing the information encoded in a collection of two-level quantum-mechanical systems – qubits – quantum analogs of classical bits. Such a computer would typi-

---

\*E-mail: dap@iesl.forth.gr

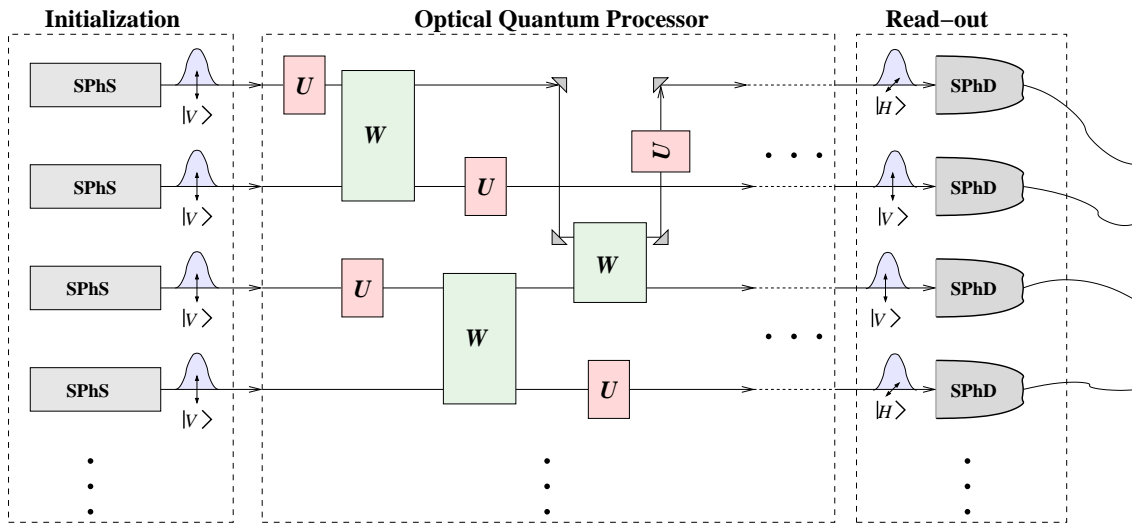


FIG. 1: Schematic representation of the quantum computer with single-photon qubits. The operation of the computer consists of the following principal steps: *Qubit initialization* is realized by deterministic single-photon sources (SPhS). *Information processing* is implemented by the quantum processor with single-qubit  $U$  and two-qubit  $W$  logic gates. *Read-out* of the result of computation is accomplished by efficient single-photon detectors (SPhD).

cally be composed of (a) quantum register containing a number of qubits, whose computational basis states are labeled as  $|0\rangle$  and  $|1\rangle$ ; (b) one- and two-qubit (and possibly multi-qubit) logic gates – unitary operations applied to the register according to the particular algorithm; and (c) measuring apparatus applied to the desired qubits at the end of (and, possibly, during) the program execution, which project the qubit state onto the computational basis  $\{|0\rangle, |1\rangle\}$ . Operation of the quantum computer may formally be divided into the following principal steps. *Initialization*: Preparation of all qubits of the register in a well-defined initial state, such as, e.g.,  $|0\dots 000\rangle$ . *Input*: Loading the input data using the logic gates. *Computation*: The desired unitary transformation of the register. Any multiqubit unitary transformation can be decomposed into a sequence of single-qubit rotations and two- (or more) qubit conditional operations, which thus constitute the universal set of quantum logic gates. *Output*: Projective measurement of the final state of the register in the computational basis. The reliable measurement scheme would need to have the fidelity more than  $1/2$ , but ideally as close to 1 as possible.

A schematic representation of an optical quantum computer is shown in figure 1. In the initialization section of the computer, deterministic sources of single photons generate single-photon pulses with precise timing and well-defined polarization and pulse-shapes (see section V). A collection of such photons constitutes the quantum register. The qubit basis states  $\{|0\rangle, |1\rangle\}$  of the register are represented by the vertical  $|V\rangle \equiv |0\rangle$  and horizontal  $|H\rangle \equiv |1\rangle$  polarization states of the photons. The preparation of an initial state of the register and the execution of the program according to the desired quantum algorithm is implemented by the quantum processor. This amounts to the application of certain sequence

of single-qubit  $U$  and two-qubit  $W$  unitary operations, whose physical realization is described below. Finally, the result of computation is read-out by a collection of efficient polarization-sensitive photon detectors (see section VII).

For the photon-polarization qubit  $|\psi\rangle = \alpha|V\rangle + \beta|H\rangle$ , the universal set of quantum gates can be constructed from arbitrary single-qubit rotation operations  $U$  and a two-qubit conditional operation  $W$ , such as the controlled-NOT (CNOT) operation  $|a\rangle|b\rangle \rightarrow |a\rangle|a \oplus b\rangle$  ( $a, b \in \{0, 1\}$ ) or controlled-phase or  $Z$  (CPHASE or CZ) operation  $|a\rangle|b\rangle \rightarrow (-1)^{ab}|a\rangle|b\rangle$ . In turn, any single-qubit unitary operation  $U$  can be decomposed into a product of rotation  $R(\theta)$  and phase-shift  $T(\phi)$  operations

$$R(\theta) = \begin{bmatrix} \cos \theta & -\sin \theta \\ \sin \theta & \cos \theta \end{bmatrix}, \quad T(\phi) = \begin{bmatrix} 1 & 0 \\ 0 & e^{i\phi} \end{bmatrix},$$

and an overall phase shift  $e^{i\varphi}$ . As an example, the Pauli  $X, Y, Z$  and Hadamard  $H$  transformations can be represented as  $X = R(\pi/2)T(\pi)$ ,  $Y = e^{i\pi/2}R(\pi/2)$ ,  $Z = T(\pi)$ ,  $H = R(\pi/4)T(\pi)$ .

As shown in figure 2(a), for the photon-polarization qubit  $|\psi\rangle$  the  $R(\theta)$  and  $T(\phi)$  operations are implemented, respectively, by the rotation of photon polarization by angle  $\theta$  about the propagation direction, and relative phase-shift  $\phi$  of the  $|V\rangle$  and  $|H\rangle$  polarized components of the photon. Both operations are easy to implement with the standard linear optical elements, Faraday rotators, polarizing beam-splitters or phase-retardation (birefringent) waveplates. A possible realization of the CPHASE two-qubit entangling operation is shown in figure 2(b). There, after passing through a polarizing beam-splitter, the vertically polarized component of each photon is transmitted, while the horizontally polarized component is di-

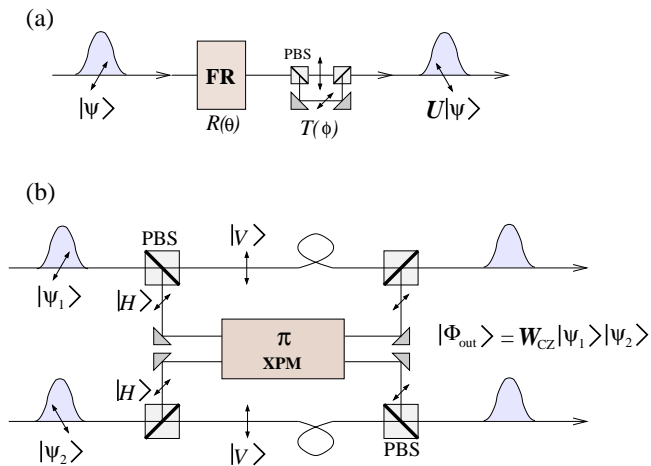


FIG. 2: Proposed physical implementation of quantum logic gates. (a) Single-qubit logic gates  $U$  are implemented with a sequence of two linear-optics operations:  $R(\theta)$  – Faraday rotation (FR) of photon polarization by angle  $\theta$  of the propagation direction;  $T(\phi)$  – relative phase-shift  $\phi$  of the photon’s  $|V\rangle$  and  $|H\rangle$  polarized components due to their optical paths difference. (b) Two-qubit CZ (or CPHASE) gate  $W_{CZ}$  is realized using polarizing beam-splitters (PBS) and  $\pi$  cross-phase modulation studied in section VI.

rected into the active medium, wherein the two-photon state  $|\Phi_{in}\rangle = |H_1 H_2\rangle$  acquires the conditional phase-shift  $\pi$ , as discussed in section VI. At the output, each photon is recombined with its vertically polarized component on another polarizing beam-splitter, where the complete temporal overlap of the vertically and horizontally polarized components of each photon is achieved by delaying the  $|V\rangle$  wavepacket in a fiber loop or sending it through a EIT vapor cell in which the pulse propagates with a reduced group velocity (see section III).

The remainder of this paper is devoted to the physical realizations of the constituent parts of the optical quantum computer described above.

### III. ELECTROMAGNETICALLY INDUCED TRANSPARENCY

The propagation of a weak probe field  $Ee^{i(kz-\omega t)}$  with carrier frequency  $\omega$  and wave vector  $k = \omega/c$  in a near-resonant medium can be characterized by the linear susceptibility  $\chi(\omega)$ , whose real and imaginary parts describe, respectively, the dispersive and absorptive properties of the medium:  $E(z) = E(0)e^{-\kappa z}e^{i\phi(z)}$ , where  $\kappa = k/2\text{Im}\chi(\omega)$  is the linear absorption coefficient, and  $\phi(z) = k/2\text{Re}\chi(\omega)z$  is the phase-shift. In the case of light interaction with two-level atoms on the transition  $|g\rangle \rightarrow |e\rangle$ , the familiar Lorentzian absorption spectrum leads to the strong attenuation of the resonant field ( $\Delta \equiv \omega - \omega_{eg} = 0$ ) in the optically dense medium according to  $E(z) = E(0)e^{-\kappa_0 z}$ , where the resonant absorption coefficient  $\kappa_0 = \sigma_0\rho$  is given by the product

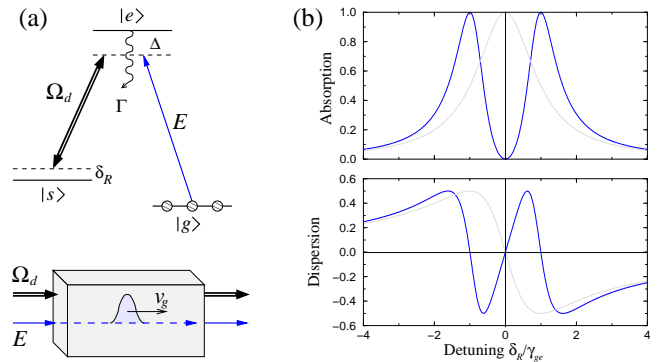


FIG. 3: Electromagnetically induced transparency in atomic medium. (a) Level scheme of three-level  $\Lambda$ -atoms interacting with a cw driving field with Rabi frequency  $\Omega_d$  on the transition  $|s\rangle \leftrightarrow |e\rangle$  and a weak pulsed  $E$  field acting on the transition  $|g\rangle \leftrightarrow |e\rangle$ . The lower states  $|g\rangle$  and  $|s\rangle$  are long-lived (metastable), while the excited state  $|e\rangle$  decays fast with the rate  $\Gamma$ . (b) Absorption and dispersion spectra ( $\delta_R = \Delta$ ) of the atomic medium for the  $E$  field in units of resonant absorption coefficient  $\kappa_0$ , for  $\Omega_d/\gamma_{ge} = 1$  and  $\gamma_R/\gamma_{ge} = 10^{-3}$ . The light-gray curves correspond to the case of  $\Omega_d = 0$  (two-level atom).

of atomic density  $\rho$  and absorption cross-section  $\sigma_0 = \wp_{ge}^2\omega/(2\hbar c\epsilon_0\gamma_{ge})$ ,  $\wp_{ge} = \langle g|\mathbf{d}|e\rangle$  being the dipole matrix element for the transition  $|g\rangle \rightarrow |e\rangle$  and  $\gamma_{ge}(\geq \Gamma/2)$  the corresponding coherence relaxation rate. When, however, the excited state  $|e\rangle$  having decay rate  $\Gamma$  is coupled by a strong driving field with Rabi frequency  $\Omega_d$  and detuning  $\Delta_d = \omega_d - \omega_{es}$  to a third metastable state  $|s\rangle$ , the situation changes dramatically (figure 3(a)). Assuming all the atoms initially reside in state  $|g\rangle$ , the complex susceptibility now takes the form

$$\chi(\omega) = \frac{2\kappa_0}{k} \frac{i\gamma_{ge}}{\gamma_{ge} - i\Delta + |\Omega_d|^2(\gamma_R - i\delta_R)^{-1}}, \quad (1)$$

where  $\delta_R = \Delta - \Delta_d = \omega - \omega_d - \omega_{sg}$  is the two-photon Raman detuning and  $\gamma_R$  the Raman coherence (spin) relaxation rate. Obviously, in the limit of  $\Omega_d \rightarrow 0$ , the susceptibility (1) reduces to that for the two-level atom. The absorption and dispersion spectra corresponding to the susceptibility of equation (1) are shown in figure 3(b) for the case of  $\Omega_d = \gamma_{ge}$  and  $\Delta_d = 0$ , i.e.  $\delta_R = \Delta$ . As seen, the interaction with the driving field results in the Autler-Townes splitting of the absorption spectrum into two peaks separated by  $2\Omega_d$ , while at the line center the medium becomes transparent to the resonant field, provided  $\gamma_R \ll |\Omega_d|^2/\gamma_{ge}$ . This effect is called electromagnetically induced transparency (EIT) [10, 11]. At the exit from the optically dense medium of length  $L$  (optical depth  $2\kappa_0 L > 1$ ), the intensity transmission coefficient is given by  $T(\omega) = \exp[-k\text{Im}\chi(\omega)L]$ . To determine the width of the transparency window  $\delta\omega_{tw}$ , one makes a power series expansion of  $\text{Im}\chi(\omega)$  in the vicinity of max-

imum transmission  $\delta_R = 0$ , obtaining [12, 13]

$$T(\omega) \simeq \exp(-\delta_R^2/\delta\omega_{\text{tw}}^2), \quad \delta\omega_{\text{tw}} = \frac{|\Omega_d|^2}{\gamma_{ge}\sqrt{2\kappa_0 L}}, \quad (2)$$

where the usual EIT conditions,  $\Delta_d\gamma_R, \Delta_d^2\gamma_R/\gamma_{ge} \ll |\Omega_d|^2$ , are assumed satisfied. Equation (2) implies that for the absorption-free propagation, the bandwidth  $\delta\omega$  of near-resonant probe field should be within the transparency window,  $\delta\omega < \delta\omega_{\text{tw}}$ . Alternatively, the temporal width  $T$  of a Fourier-limited probe pulse should satisfy  $T \gtrsim \delta\omega_{\text{tw}}^{-1}$ .

Considering next the dispersive properties of EIT, in figure 3(b) one sees that the dispersion exhibits a steep and approximately linear slope in the vicinity of absorption minimum  $\delta_R = 0$ . Therefore, a probe field slightly detuned from the resonance by  $\delta_R < \delta\omega_{\text{tw}}$ , during the propagation would acquire a large phase-shift  $\phi(L) \simeq \kappa_0 L \gamma_{ge} \delta_R / |\Omega_d|^2$  while suffering only little absorption, as per equation (2). At the same time, a near-resonant probe pulse  $E(z, t)$  propagates through the medium with greatly reduced group velocity

$$v_g = \frac{c}{1 + c \frac{\partial}{\partial \omega} [\frac{k}{2} \text{Re}\chi(\omega)]} = \frac{c}{1 + c \frac{\kappa_0 \gamma_{ge}}{|\Omega_d|^2}} \simeq \frac{|\Omega_d|^2}{\kappa_0 \gamma_{ge}} \ll c, \quad (3)$$

while upon entering the medium, its spacial envelope is compressed by a factor of  $v_g/c \ll 1$ .

So far, we have outlined the absorptive and dispersive properties of the stationary EIT without elaborating much on the underlying physical mechanism. As elucidated below, EIT is based on the phenomenon of coherent population trapping [10, 11], in which the application of two coherent fields to a three-level  $\Lambda$  system of figure 3(a) creates the so-called ‘‘dark state’’, which is stable against absorption of both fields. Since we are interested in quantum information processing with photons, the probe field has to be treated quantum mechanically. It is expressed through the traveling-wave (multimode) electric field operator  $\hat{\mathcal{E}}(z, t) = \sum_q a^q(t) e^{iqz}$ , where  $a^q$  is the bosonic annihilation operator for the field mode with the wavevector  $k + q$ . The classical driving field with Rabi frequency  $\Omega_d$  is assumed spatially uniform. In the frame rotating with the probe and driving field frequencies, the interaction Hamiltonian has the following form:

$$H = \hbar \sum_{j=1}^N [\Delta \hat{\sigma}_{ee}^j + \delta_R \hat{\sigma}_{ss}^j - g \hat{\mathcal{E}}(z_j) e^{ikz_j} \hat{\sigma}_{eg}^j - \Omega_d(t) e^{ik_d z_j} \hat{\sigma}_{es}^j + \text{H.c.}], \quad (4)$$

where  $N = \rho V$  is the total number of atoms in the quantization volume  $V = AL$  ( $A$  being the cross-sectional area of the probe field),  $\hat{\sigma}_{\mu\nu}^j = |\mu_j\rangle\langle\nu_j|$  is the transition operator of the  $j$ th atom at position  $z_j$ ,  $k_d$  is the projection of the driving field wavevector onto the  $\mathbf{e}_z$  direction, and  $g = \frac{\varrho_{ge}}{\hbar} \sqrt{\frac{\hbar\omega}{2\epsilon_0 V}}$  is the atom-field coupling constant. For

$\delta_R = 0$ , the Hamiltonian (4) has a family of dark eigenstates  $|D_n^q\rangle$  with zero eigenvalue  $H|D_n^q\rangle = 0$ , which are decoupled from the rapidly decaying excited state  $|e\rangle$ :

$$|D_n^q\rangle = \sum_{m=0}^n \binom{n}{m}^{\frac{1}{2}} (-\sin\theta)^m (\cos\theta)^{n-m} |(n-m)^q\rangle |s^{(m)}\rangle. \quad (5)$$

Here the mixing angle  $\theta(t)$  is defined via

$$\tan^2\theta(t) = \frac{g^2 N}{|\Omega_d(t)|^2},$$

$|n^q\rangle$  denotes the state of the quantum field with  $n$  photons in mode  $q$ , and  $|s^{(m)}\rangle$  is a symmetric Dicke-like state of the atomic ensemble with  $m$  Raman (spin) excitations, i.e., atoms in state  $|s\rangle$ , defined as

$$\begin{aligned} |s^{(0)}\rangle &\equiv |g_1, g_2, \dots, g_N\rangle, \\ |s^{(1)}\rangle &\equiv \frac{1}{\sqrt{N}} \sum_{j=1}^N e^{i(k+q-k_d)z_j} |g_1, \dots, s_j, \dots, g_N\rangle, \\ |s^{(2)}\rangle &\equiv \frac{1}{\sqrt{2N(N-1)}} \sum_{i \neq j=1}^N e^{i(k+q-k_d)(z_i+z_j)} \\ &\quad \times |g_1, \dots, s_i, \dots, s_j, \dots, g_N\rangle, \end{aligned}$$

etc. When  $\theta = 0$  ( $|\Omega_d|^2 \gg g^2 N$ ), the dark state (5) is comprised of purely photonic excitation,  $|D_n^q\rangle = |n^q\rangle |s^{(0)}\rangle$ , while in the opposite limit of  $\theta = \pi/2$  ( $|\Omega_d|^2 \ll g^2 N$ ), it coincides with the collective atomic excitation  $|D_n^q\rangle = (-1)^n |0^q\rangle |s^{(n)}\rangle$ . For intermediate values of mixing angle  $0 < \theta < \pi/2$ , the dark state represents a coherent superposition of photonic and atomic Raman excitations [16, 26]. Below will be concerned with the case of single-photon probe field, for which the dark state takes a particularly simple form

$$|D_1^q\rangle = \cos\theta |1^q, s^{(0)}\rangle - \sin\theta |0^q, s^{(1)}\rangle. \quad (6)$$

Consider now the dynamic evolution of the field and atomic operators. In the slowly varying envelope approximation, the propagation equation for the quantum field has the form

$$\left( \frac{\partial}{\partial t} + c \frac{\partial}{\partial z} \right) \hat{\mathcal{E}}(z, t) = igN \hat{\sigma}_{ge}, \quad (7)$$

where  $\hat{\sigma}_{\mu\nu}(z, t) = \frac{1}{N_z} \sum_{j=1}^{N_z} \hat{\sigma}_{\mu\nu}^j$  is the collective atomic operator averaged over small but macroscopic volume containing many atoms  $N_z = (N/L)dz \gg 1$  around position  $z$ . The evolution of the atomic operators is governed by a set of Heisenberg-Langevin equations [16], which are treated perturbatively in the small parameter  $g\hat{\mathcal{E}}/\Omega_d$  and in the adiabatic approximation for both fields,

$$\hat{\sigma}_{ge} = -\frac{i}{\Omega_d^*} \left[ \frac{\partial}{\partial t} - i\delta_R + \gamma_R \right] \hat{\sigma}_{gs} + \frac{i}{\Omega_d^*} \hat{F}_{gs}, \quad (8a)$$

$$\hat{\sigma}_{gs} = -\frac{g\hat{\mathcal{E}}}{\Omega_d} \left[ 1 + \frac{\delta_R(\Delta + i\gamma_{ge})}{|\Omega_d|^2} \right] + \frac{i}{\Omega_d} \hat{F}_{ge}, \quad (8b)$$

where  $\hat{F}_{\mu\nu}$  are  $\delta$ -correlated noise operators associated with the atomic relaxation. When the driving field is constant in time and  $\delta_R \Delta \ll |\Omega_d|^2$ , equations (7-8) yield

$$\left( \frac{\partial}{\partial z} + \frac{1}{v_g} \frac{\partial}{\partial t} \right) \hat{\mathcal{E}} = -\kappa \hat{\mathcal{E}} + i s \delta_R \hat{\mathcal{E}} + \hat{\mathcal{F}}, \quad (9)$$

where  $v_g = c \cos^2 \theta$  is the group velocity of (3), while  $\kappa = \tan^2 \theta / c (\gamma_R + \gamma_{ge} \delta_R^2 / |\Omega_d|^2)$  and  $s = \tan^2 \theta / c$  are, respectively, the linear absorption and phase-modulation coefficients. The solution of equation (9) can be expressed in terms of the retarded time  $\tau = t - z/v_g$  as

$$\hat{\mathcal{E}}(z, t) = \hat{\mathcal{E}}(0, \tau) \exp[-\kappa z + i\phi(z)] + \hat{\mathcal{F}}, \quad (10)$$

with  $\phi(z) = s \delta_R z$  (the noise operator  $\hat{\mathcal{F}}$  ensures the conservation of field commutators [27]). We will be interested in the input states corresponding to single-photon wavepackets  $|1\rangle = \sum_q \xi^q |1^q\rangle$  ( $|1^q\rangle = a^{q\dagger} |0\rangle$ ), where the Fourier amplitudes  $\xi^q$ , normalized as  $\sum_q |\xi^q|^2 = 1$ , define the spatial envelope  $f(z)$  of the probe pulse that initially (at  $t = 0$ ) is localized around  $z = 0$ ,

$$\langle 0 | \hat{\mathcal{E}}(z, 0) | 1 \rangle = \sum_q \xi^q e^{iqz} = f(z).$$

In free space,  $\hat{\mathcal{E}}(z, t) = \hat{\mathcal{E}}(0, \tau)$  with  $\tau = t - z/c$ , and we have  $\langle 0 | \hat{\mathcal{E}}(z, t) | 1 \rangle = f(z - ct)$ . Upon propagating through the EIT medium, using equation (10) and neglecting the (small) absorption, for the expectation value of the probe field intensity  $\langle \hat{I}(z, t) \rangle = \langle 1 | \hat{\mathcal{E}}^\dagger(z, t) \hat{\mathcal{E}}(z, t) | 1 \rangle$  one has

$$\langle \hat{I}(z, t) \rangle = |f(-c\tau)|^2 = |f(zc/v_g - ct)|^2, \quad (11)$$

where  $\tau = t - z/v_g$  for  $0 \leq z < L$ . This equation indicates that at the entrance to the medium, as the group velocity of the pulse is slowed down to  $v_g$ , its spatial envelope is compressed by a factor of  $v_g/c \ll 1$ . Outside the medium, at  $z \geq L$  and accordingly  $\tau = t - L/v_g - (z - L)/c$ , one has  $\langle \hat{I}(z, t) \rangle = |f(z + L(c/v_g - 1) - ct)|^2$ , which shows that the propagation velocity and the pulse envelope are restored to their free-space values.

Consider finally the case of the exact two-photon Raman resonance  $\delta_R = 0$  and time-dependent driving field  $\Omega_d(t)$ . To solve the coupled set of equations (7-8), one introduces a polariton operator [16]

$$\hat{\Psi}(z, t) = \cos \theta(t) \hat{\mathcal{E}}(z, t) - \sin \theta(t) \sqrt{N} \hat{\sigma}_{gs}, \quad (12)$$

whose photonic and atomic components are determined by the mixing angle  $\theta$ ,  $\hat{\mathcal{E}} = \cos \theta \hat{\Psi}$  and  $\hat{\sigma}_{gs} = \sin \theta \hat{\Psi} / \sqrt{N}$ . Taking the plain-wave decomposition of the polariton operator  $\hat{\Psi}(z, t) = \sum_q \hat{\psi}^q(t) e^{iqz}$ , one can show that in the weak-field limit the mode operators  $\hat{\psi}^q$  obey the bosonic commutation relations  $[\hat{\psi}^q, \hat{\psi}^{q'\dagger}] = \delta_{qq'}$  [16]. Moreover,

by acting  $n$  times with operator  $\hat{\psi}^{q\dagger}$  onto the state  $|0^q\rangle |s^{(0)}\rangle$  one creates the dark state of (5),

$$|D_n^q\rangle = \frac{1}{\sqrt{n!}} (\hat{\psi}^{q\dagger})^n |0^q\rangle |s^{(0)}\rangle.$$

Therefore the operator  $\hat{\Psi}$  had been called dark-state polariton [16]. It is easy to verify that upon neglecting the absorption, the equation of motion for  $\hat{\Psi}(z, t)$  takes a particularly simple form

$$\left( \frac{\partial}{\partial t} + v_g(t) \frac{\partial}{\partial z} \right) \hat{\Psi}(z, t) = 0. \quad (13)$$

Its solution is given by

$$\hat{\Psi}(z, t) = \hat{\Psi} \left( z - \int_0^t v_g(t') dt', 0 \right), \quad (14)$$

which describes a state- and shape-preserving pulse propagation with time-dependent group velocity  $v_g(t) = c \cos^2 \theta(t)$ . Thus, once the pulse has fully accommodated in the medium, one can stop it by adiabatically rotating the mixing angle from its initial value  $0 \leq \theta < \pi/2$  to  $\theta = \pi/2$ , which amounts to switching off the driving field  $\Omega_d$ . As a result, the state of the photonic component of the pulse is coherently mapped onto the collective atomic state according to (5) or (6), the latter applies to a single-photon input pulse. In order to accommodate the pulse in the medium with negligible losses, its duration should exceed the inverse of the initial EIT bandwidth, while at the entrance its length should be compressed to the length of the medium,  $\delta \omega_{\text{tw}}^{-1} v_g \ll T v_g < L$ . These two conditions yield  $(2\kappa_0 L)^{-1/2} \ll T v_g / L < 1$ , which requires media with large optical depth  $2\kappa_0 L \gg 1$ . Note finally, that although the collective state  $|s^{(1)}\rangle$  is an entangled state of  $N$  atoms, it decoheres with essentially single-atom rate and is quite stable against one (or few) atom losses [28]. Therefore the coherent trapping time is limited mainly by the life-time of Raman coherence  $\gamma_R^{-1}$ .

#### IV. PHOTONIC MEMORY

With straightforward modifications, the technique described above can be used to realize a reversible memory device for the photon-polarization qubit. To that end, after passing through a  $\lambda/4$  plate oriented at  $45^\circ$ , the vertically- and horizontally-polarized components of the single-photon pulse are converted into the circularly right- and left-polarized ones according to  $|V\rangle \rightarrow |R\rangle = \frac{1}{\sqrt{2}}(|V\rangle + i|H\rangle)$  and  $|H\rangle \rightarrow |L\rangle = \frac{1}{\sqrt{2}}(|V\rangle - i|H\rangle)$ . The pulse is then sent to the atomic medium with M-level configuration, as shown in figure 4. All the atoms are initially prepared in the ground state  $|g\rangle$ , the  $E_{L,R}$  components of the field interact with the atoms on the corresponding transitions  $|g\rangle \rightarrow |e_{1,2}\rangle$ , while the excited states  $|e_{1,2}\rangle$  are coupled to the metastable states  $|s_{1,2}\rangle$  via the same driving field with Rabi frequency  $\Omega_d$ . Once

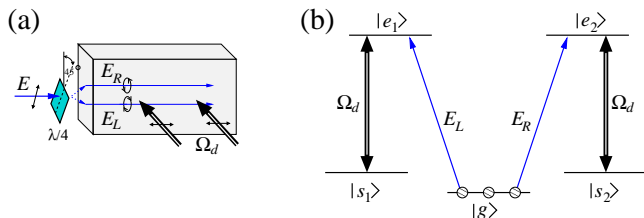


FIG. 4: Reversible memory for the photon-polarization qubit. (a) After the basis transformation  $|V\rangle \rightarrow |R\rangle$ ,  $|H\rangle \rightarrow |L\rangle$  on a  $45^\circ$  oriented  $\lambda/4$  plate, the photon enters the atomic medium serving as a memory device. (b) Level scheme of M-atoms interacting with the  $E_{L,R}$  components of single-photon pulse and the driving field with Rabi frequency  $\Omega_d$ .

the pulse has fully accommodated in the medium, the driving field  $\Omega_d$  is adiabatically switched off. As a result, the photon wavepacket is stopped in the medium, and its state  $|\psi\rangle$  is coherently mapped onto the collective atomic state according to [26, 28]

$$\alpha |L\rangle + \beta |R\rangle \rightarrow \alpha |s_1^{(1)}\rangle + \beta |s_2^{(1)}\rangle. \quad (15)$$

This collective state is stable against decoherence [28], allowing for a long storage time of the qubit state in the atomic ensemble. At a later time, the photon can be released from the medium on demand by switching the driving field on, which results in the reversal of mapping (15).

## V. DETERMINISTIC SOURCE OF SINGLE-PHOTONS

Generation of single-photons in a well defined spatiotemporal mode is a challenging task that is currently attracting much effort [29]. In a simplest setup, one typically employs spontaneous parametric down conversion [30] to generate a pair of polarization- and momentum-correlated photons. Then, conditional upon the outcome of measurement on one of the photons, the other photon is projected onto a well-defined polarization and momentum state. In more elaborate experiments, single emitters, such as quantum dots [31] or molecules [32], emit single photons at a time when optically pumped into an excited state. Recently, truly deterministic sources of single photons have been realized with single atoms in high- $Q$  optical cavities [33]. In these experiments, single-photon wavepackets with precise propagation direction and well characterized timing and temporal shape were generated using the technique of intracavity stimulated Raman adiabatic passage (STIRAP). Notwithstanding these achievements, the cavity QED experiments in the strong coupling regime required by the intracavity STIRAP involve sophisticated experimental setup which is very difficult, if not impossible, to scale up to a large number of independent emitters operating in parallel.

In this section, we describe a method for deterministic

generation of single-photon pulses from coherently manipulated atomic ensembles. As discussed in section III, symmetric Raman (spin) excitations in optically thick atomic medium exhibit collectively enhanced coupling to light in the EIT regime; Once the single excitation state  $|s^{(1)}\rangle$  is created in the medium, the application of resonant driving field  $\Omega_d$  on the transition  $|s\rangle \rightarrow |e\rangle$  will stimulate the Raman transition  $|s\rangle \rightarrow |g\rangle$  and produce a single-photon anti-Stokes pulse  $E$ , whose propagation direction and pulse-shape are completely determined by the driving-field parameters. The question is then: How can one produce, in a deterministic fashion, precisely one collective Raman excitation? In a number of recent theoretical and experimental studies, such excitations were produced by the process of spontaneous Raman scattering. Namely, one applies a classical pump laser to the atomic transition  $|g\rangle \rightarrow |e\rangle$  and detects the number of forward scattered Stokes photons [34]. Since the emission of each such photon results in one atomic excitation  $|s\rangle$  symmetrically distributed in the whole ensemble, the number of Stokes photons is uniquely correlated with the number of Raman excitations of the medium. However, due to the spontaneous nature of the scattering process, the production of collective single excitation state  $|s^{(1)}\rangle$  requires the postselection conditioned upon the measured number of Stokes photons, which makes this scheme essentially probabilistic

Below we will describe a scheme that is capable of producing the single collective Raman excitation at a time. It is based on the dipole-blockade technique proposed in [35], which employs the exceptionally strong dipole-dipole interactions between pairs of Rydberg atoms. In a static electric field  $E_{st}e_z$ , the linear Stark effect results in splitting of highly excited Rydberg states into a manifold of  $2n - 1$  states with energy levels  $\hbar\Delta\nu_{nqm} = \frac{3}{2}nqea_0E_{st}$ , where  $n$  is the principal quantum number,  $q \equiv n_1 - n_2 = n - 1 - |m|, n - 3 - |m|, \dots, -(n - 1 - |m|)$ , and  $m = n - 1, n - 2, \dots, -(n - 1)$  are, respectively, parabolic and magnetic quantum numbers,  $e$  is the electron charge, and  $a_0$  is the Bohr radius [36]. These Stark eigenstates possess large permanent dipole moments  $\mathbf{d} = \frac{3}{2}nqea_0e_z$ . A pair of atoms 1 and 2 prepared in such Stark eigenstates  $|r\rangle$  interact with each other via the dipole-dipole potential

$$V_{DD} = \frac{\mathbf{d}_1 \cdot \mathbf{d}_2 - 3(\mathbf{d}_1 \cdot \mathbf{e}_{12})(\mathbf{d}_2 \cdot \mathbf{e}_{12})}{4\pi\epsilon_0 R^3}, \quad (16)$$

where  $\mathbf{R} = R\mathbf{e}_{12}$  is the distance between the atoms. The dipole-dipole interaction (16) results in an energy shift of the pair of Rydberg atoms, as well as their coupling to the other Stark eigenstates within the same  $n$  manifold, which in turn splits the energy levels  $|r\rangle$ .

Consider next a dense ensemble of double- $\Lambda$  atoms shown in figure 5. A coherent laser field with Rabi frequency  $\Omega_r^{(1)} < \Delta\nu$  resonantly couples the initial atomic state  $|g\rangle$  to the selected Stark eigenstate  $|r\rangle$ , while the second resonant field acts on the transition  $|r\rangle \rightarrow |s\rangle$  with Rabi frequency  $\Omega_r^{(2)}$ . When  $\Omega_d = E = 0$ , one can

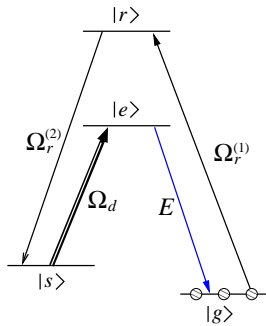


FIG. 5: Level scheme of atoms for deterministic generation of single-photons. Dipole-dipole interaction between pairs of atoms in Rydberg states  $|r\rangle$  facilitates the generation of single collective Raman excitation of the atomic ensemble at a time, via the sequential application of the  $\Omega_r^{(1)}$  and  $\Omega_r^{(2)}$  pulses of (effective) area  $\pi$ . This collective excitation is then adiabatically converted into a single-photon wavepacket by switching on the driving field  $\Omega_d$ .

disregard state  $|e\rangle$ , and the Hamiltonian takes the form

$$H = V_{\text{AF}} + V_{\text{DD}}, \quad (17)$$

with the atom-field and dipole-dipole interaction terms given, respectively, by

$$V_{\text{AF}} = -\hbar \sum_j^N [\Omega_r^{(1)} e^{ik_r^{(1)} z_j} \hat{\sigma}_{rg}^j + \Omega_r^{(2)} e^{ik_r^{(2)} z_j} \hat{\sigma}_{rs}^j + \text{H.c.}], \quad (18a)$$

$$V_{\text{DD}} = \hbar \sum_{i>j}^N \Delta_{ij}(R) |r_i r_j\rangle \langle r_i r_j|, \quad (18b)$$

where  $\Delta_{ij}(R) = \langle r_i r_j | V_{\text{DD}} | r_i r_j \rangle \approx -n^4 e^2 a_0^2 / (\pi \hbar \epsilon_0 R^3)$  is the dipole-dipole energy shift for a pair of atoms  $i$  and  $j$  separated by distance  $R$ . Suppose that initially all the atoms are in state  $|g\rangle$ , while the second laser is switched off,  $\Omega_r^{(2)} = 0$ . Then the first laser field, coupled symmetrically to all the atoms, will induce the transition from the ground state  $|g_1, g_2, \dots, g_N\rangle \equiv |s^{(0)}\rangle$  to the collective state  $|r^{(1)}\rangle \equiv \frac{1}{\sqrt{N}} \sum_j e^{ik_r^{(1)} z_j} |g_1, \dots, r_j, \dots, g_N\rangle$  representing a symmetric single Rydberg excitation of the atomic ensemble. The collective Rabi frequency on the transition  $|s^{(0)}\rangle \rightarrow |r^{(1)}\rangle$  is  $\sqrt{N} \Omega_r^{(1)}$ . Once an atom  $i \in \{1, \dots, N\}$  is excited to the state  $|r\rangle$ , the excitation of a second atom  $j (\neq i)$  is constrained by the dipole-dipole interaction between the atoms: Provided  $|\Delta_{ij}| > \Omega_r^{(1)}, \gamma_r$ , where  $\gamma_r$  is the width of level  $|r\rangle$ , the nonresonant transitions  $|r_i g_j\rangle \rightarrow |r_i r_j\rangle$  resulting in two-atom excitations are suppressed. Hence, applying a laser pulse of area  $\sqrt{N} \Omega_r^{(1)} T = \pi/2$  (an effective  $\pi$  pulse), one produces the single Rydberg excitation state  $|r^{(1)}\rangle$ . At the end of the pulse, the probability of error due to populating the doubly-excited states  $|r_i r_j\rangle$  is found by adding

the probabilities of all possible double-excitations,

$$P_{\text{double}} \sim \frac{1}{N} \sum_{i,j} \frac{|\Omega_r^{(1)}|^2}{\Delta_{ij}^2} \approx \frac{N |\Omega_r^{(1)}|^2}{\bar{\Delta}^2}.$$

Thus  $P_{\text{double}} \ll 1$  when the collective Rabi frequency  $\sqrt{N} \Omega_r^{(1)}$  is small compared to the average dipole-dipole energy shift  $\bar{\Delta}$ . Another source of errors is the dephasing given by  $P_{\text{deph}} \leq \gamma_r T \sim \gamma_r / (\sqrt{N} \Omega_r^{(1)})$ , which is typically very small for long-lived Rydberg states and  $N \gg 1$ . By the subsequent application of the second laser with the area  $\Omega_r^{(2)} T = \pi/2$  ( $\pi$  pulse), the state  $|r^{(1)}\rangle$  can be converted into the symmetric Raman excitation state  $|s^{(1)}\rangle \equiv \frac{1}{\sqrt{N}} \sum_j e^{i(k_r^{(1)} - k_r^{(2)}) z_j} |g_1, \dots, s_j, \dots, g_N\rangle$ , which is precisely the state we need for the generation of single-photon pulse, as described above.

To relate the foregoing discussion to a realistic experiment, let us assume cold alkali atoms (Rb) loaded into an elongated trap of length  $L \simeq 10 \mu\text{m}$  and cross-section  $A \simeq 10 \mu\text{m}^2$ . The Stark eigenstates are resonantly selected from within the Rydberg states with the effective principal quantum number  $n \simeq 50$ . The dipole-dipole energy shift is smallest for pairs of atoms located at the opposite ends of the trap,  $\bar{\Delta} \gtrsim \Delta_{ij}(L) \sim 2\pi \times 20 \text{ MHz}$ . For the density  $\rho \simeq 10^{14} \text{ cm}^{-3}$ , the trap contains  $N \simeq 10^4$  atoms, and the (single atom) Rabi frequency should be chosen as  $\Omega_r^{(1)} \leq 2\pi \times 100 \text{ kHz}$ . Then, for the preparation time  $T \sim 0.1 \mu\text{s}$  of state  $|s^{(1)}\rangle$ , the achievable fidelity is  $\gtrsim 98\%$ . For these parameters, the optical depth of the medium is large,  $2\kappa_0 L \simeq 100$ , which is necessary for efficient generation of single-photon pulses by switching on the driving field  $\Omega_d$  and converting the atomic Raman excitation into the photonic excitation, as discussed in section III.

It should be mentioned that a related scheme for single photon generation employing the dipole blockade technique was proposed in [37]. There, however, a single atom at a time was transferred to an excited state, from where it spontaneously decayed back to the ground state producing a single fluorescent photon in a well-defined direction.

## VI. PHOTON-PHOTON INTERACTION

Conventional media are typically characterized by weak optical nonlinearities, which are manifest only at high intensities of electromagnetic fields [9] and are vanishingly small for single- or few-photon fields. It was first pointed out in [20], however, that the ultrahigh sensitivity of EIT dispersion to the two-photon Raman detuning  $\delta_R$  in the vicinity of absorption minimum, can be used to achieve giant Kerr nonlinearities between two weak optical fields interacting with four-level atoms in N-configuration of levels. As was shown in section III, a probe field with  $\delta_R = 0$  propagating in the EIT medium experiences negligible absorption and phase-shift. When,

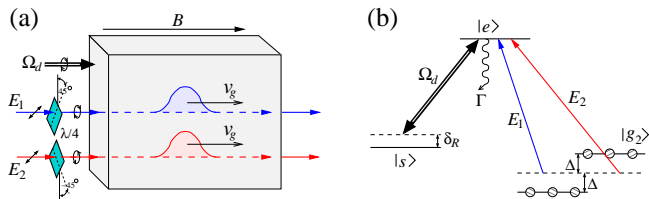


FIG. 6: Cross-phase modulation of two single-photon pulses. (a) Two horizontally polarized photons  $E_1$  and  $E_2$ , after passing through the  $\pm 45^\circ$  oriented  $\lambda/4$  plates, are converted into the circularly left- and right-polarized photons, which are sent into the active medium. (b) Level scheme of tripod atoms interacting with quantum fields  $E_{1,2}$ , strong cw driving field with Rabi frequency  $\Omega_d$  and weak magnetic field  $B$  that removes the degeneracy of Zeeman sublevels  $|g_1\rangle$  and  $|g_2\rangle$ .

however, a second weak (signal) field, dispersively coupling state  $|s\rangle$  to another excited state  $|f\rangle$ , is introduced in the medium, it causes a Stark shift of level  $|s\rangle$ , given by  $\Delta_{St} = |\Omega_s|^2/\Delta_s$ , where  $\Omega_s$  is the Rabi frequency and  $\Delta_s > \Omega_s, \Gamma_f$  is the detuning of the signal field from the  $|s\rangle \rightarrow |f\rangle$  resonance. Thus the EIT spectrum is effectively shifted by the amount of  $\Delta_{St}$ , which results in the conditional phase-shift of the probe field,  $\phi(z) \simeq \kappa_0 z \gamma_{ge} \Delta_{St}/|\Omega_d|^2$ . Notwithstanding this promising sensitivity, large conditional phase shift of one weak (single-photon) pulse in the presence of another (also known as cross-phase modulation) faces serious challenges in spatially uniform media. In order to eliminate the two-photon absorption [21] associated with Doppler broadening  $\delta\omega_D$  of the atomic resonance  $|s\rangle \rightarrow |f\rangle$ , one either has to work with cold atoms, or choose large detuning  $\Delta_s > \delta\omega_D$ , which limits the resulting cross-phase shift. Another drawback of this scheme is the mismatch between the slow group velocity of the probe pulse subject to EIT, and that of the nearly-free propagating signal pulse, which severely limits their effective interaction length and the maximal conditional phase-shift [22]. This drawback may be remedied by using an equal mixture of two isotopic species, interacting with two driving fields and an appropriate magnetic field, which would render the group velocities of the two pulses equal [23]. Other schemes to achieve the group velocity matching and strong cross-phase modulation were proposed in [38, 39, 40]. Here we discuss an alternative, simple and robust approach [27], in which two weak (single-photon) fields, propagating through a medium of hot alkali atoms under the conditions of EIT, impress very large nonlinear phase-shift upon each other.

Consider a near-resonant interaction of two weak, orthogonally (circularly) polarized optical fields  $E_1$  and  $E_2$  and a strong driving field with Rabi frequency  $\Omega_d$  with a medium of atoms having tripod configuration of levels, as shown in figure 6. The medium is subject to a weak longitudinal magnetic field  $B$  that removes the degeneracy of the ground state sublevels  $|g_1\rangle$  and  $|g_2\rangle$ , whose Zeeman shift is given by  $\hbar\Delta = \mu_B m_F g_F B$ , where  $\mu_B$  is

the Bohr magneton,  $g_F$  is the gyromagnetic factor and  $m_F = \pm 1$  is the magnetic quantum number of the corresponding state. All the atoms are assumed to be optically pumped to the states  $|g_1\rangle$  and  $|g_2\rangle$ , which thus have the same incoherent populations  $\langle \hat{\sigma}_{g_1 g_1} \rangle = \langle \hat{\sigma}_{g_2 g_2} \rangle = 1/2$ . The weak fields  $E_1$  and  $E_2$ , having the same carrier frequency  $\omega = \omega_{eg}^0$  equal to the  $|g_{1,2}\rangle \rightarrow |e\rangle$  resonance frequency for zero magnetic field, and wavevector  $k$  parallel to the magnetic field direction, act on the atomic transitions  $|g_1\rangle \rightarrow |e\rangle$  and  $|g_2\rangle \rightarrow |e\rangle$ , with the detunings  $\delta_{1,2} = \mp \Delta - kv$ , where  $kv$  is the Doppler shift for the atoms having velocity  $v$  along the propagation direction. In the collinear Doppler-free geometry shown in figure 6(a), the circularly polarized driving field couples level  $|e\rangle$  to a single magnetic sublevel  $|s\rangle$ , whose Zeeman shift  $\hbar\Delta' = \mu_B m_{F'} g_{F'} B$  is incorporated in the driving field detuning,  $\delta_d = \omega_d - \omega_{es}^0 + \Delta' - kv = \Delta_d - kv$ .

Assuming, as before, the weak-field limit and adiabatically eliminating the atomic degrees of freedom, the equations of motion for the electric field operators  $\hat{\mathcal{E}}_{1,2}$  corresponding to the quantum fields  $E_{1,2}$  are obtained as [27]

$$\left(\frac{\partial}{\partial z} + \frac{1}{v_g} \frac{\partial}{\partial t}\right) \hat{\mathcal{E}}_1 = -\kappa_1 \hat{\mathcal{E}}_1 - i(\Delta + \Delta_d)(s_1 - \eta_1 \hat{I}_2) \hat{\mathcal{E}}_1 + \hat{\mathcal{F}}_1, \quad (19a)$$

$$\left(\frac{\partial}{\partial z} + \frac{1}{v_g} \frac{\partial}{\partial t}\right) \hat{\mathcal{E}}_2 = -\kappa_2 \hat{\mathcal{E}}_2 + i(\Delta - \Delta_d)(s_2 - \eta_2 \hat{I}_1) \hat{\mathcal{E}}_2 + \hat{\mathcal{F}}_2, \quad (19b)$$

where  $v_g = c \cos^2 \theta \ll c$  is the group velocity, with the mixing angle  $\theta$  defined as  $\tan^2 \theta = g^2 N / (2|\Omega_d|^2)$  (the factor  $1/2$  corresponds to the initial population of levels  $|g_{1,2}\rangle$ ),  $\kappa_{1,2} = \tan^2 \theta / c [\gamma_R + \gamma_{ge} (\Delta \pm \Delta_d)^2 / |\Omega_d|^2]$  and  $s_{1,2} = \tan^2 \theta / c [1 + \Delta (\Delta \pm \Delta_d) / |\Omega_d|^2]$  are, respectively, the linear absorption and phase modulation coefficients,  $\eta_{1,2} = g^2 2\Delta \tan^2 \theta / [c |\Omega_d|^2 (2\Delta \mp i\gamma_R)]$  are the cross-coupling coefficients, and  $\hat{I}_j \equiv \hat{\mathcal{E}}_j^\dagger \hat{\mathcal{E}}_j$  is the dimensionless intensity (photon-number) operator for the  $j$ th field. In deriving equations (19), the EIT conditions  $|\Omega_d|^2 \gg (\Delta + kv)(\Delta \pm \Delta_d), \gamma_R(\gamma_{ge} + kv)$ , where  $\bar{v}$  is the mean thermal atomic velocity, were assumed satisfied. Note that if states  $|g_{1,2}\rangle$  and  $|s\rangle$  belong to different hyperfine components of a common ground state, the frequencies  $\omega$  and  $\omega_d$  of the optical fields differ from each other by at most a few GHz, and the difference  $(k - k_d)v$  in the Doppler shifts of the atomic resonances  $|g_{1,2}\rangle \rightarrow |e\rangle$  and  $|s\rangle \rightarrow |e\rangle$  is negligible.

In what follows, we discuss the relatively simple case of small magnetic field, such that  $\gamma_R \ll \Delta, \Delta' \ll \Delta_d$  and  $\Delta_d = \omega_d - \omega_{es}^0$ . When absorption is negligible,  $\kappa_{1,2} z \ll 1$ ,  $z \in \{0, L\}$ , which requires that  $v_g/\gamma_R \gg L$  and  $\Delta_d^2 < \gamma_R |\Omega_d|^2 / \gamma_{ge}$ , the solution of equations (19) is

$$\hat{\mathcal{E}}_1(z, t) = \hat{\mathcal{E}}_1(0, \tau) \exp[i\eta \Delta_d \hat{\mathcal{E}}_2^\dagger(0, \tau) \hat{\mathcal{E}}_2(0, \tau) z], \quad (20a)$$

$$\hat{\mathcal{E}}_2(z, t) = \hat{\mathcal{E}}_2(0, \tau) \exp[i\eta \Delta_d \hat{\mathcal{E}}_1^\dagger(0, \tau) \hat{\mathcal{E}}_1(0, \tau) z], \quad (20b)$$

where the cross-phase modulation coefficient is given by



$\eta \simeq g^2/(v_g|\Omega_d|^2)$ , while the linear phase-modulation is incorporated into the field operators via the unitary transformations  $\hat{\mathcal{E}}_{1,2}(z, t) \rightarrow \hat{\mathcal{E}}_{1,2}(z, t)e^{i\Delta_d z/v_g}$ . The multimode field operators  $\hat{\mathcal{E}}_j(z, t) = \sum_q a_j^q(t)e^{iqz}$  ( $j = 1, 2$ ), with quantization bandwidth  $\delta q \leq \delta\omega_{\text{tw}}/c$  ( $q \in \{-\delta q/2, \delta q/2\}$ ) restricted by the width of the EIT window  $\delta\omega_{\text{tw}}$  [23], have the following equal-time commutation relations

$$[\hat{\mathcal{E}}_i(z), \hat{\mathcal{E}}_j^\dagger(z')] = \delta_{ij} \frac{L\delta q}{2\pi} \text{sinc}[\delta q(z - z')/2],$$

where  $\text{sinc}(x) = \sin(x)/x$ .

Consider the input state  $|\Phi_{\text{in}}\rangle = |1_1\rangle \otimes |1_2\rangle$ , consisting of two single photon wavepackets

$$|1_j\rangle = \sum_q \xi_j^q a_j^{q\dagger} |0\rangle = \int dz f_j(z) \hat{\mathcal{E}}_j^\dagger(z) |0\rangle \quad (j = 1, 2),$$

whose spatial envelopes  $f_j(z) = \langle 0 | \hat{\mathcal{E}}_j(z, 0) | 1_j \rangle$  are initially (at  $t = 0$ ) localized around  $z = 0$ . The state of the system at any time can be represented as

$$|\Phi(t)\rangle = \sum_{q, q'} \xi_{12}^{qq'}(t) |1_1^q\rangle |1_2^{q'}\rangle, \quad (21)$$

from where it is apparent that  $\xi_{12}^{qq'}(0) = \xi_1^q \xi_2^{q'}$ . Since for the photon-number states the expectation values of the field operators vanish, all the information about the state of the system is contained in the intensities of the corresponding fields

$$\langle \hat{I}_j(z, t) \rangle = \langle \Phi_{\text{in}} | \hat{\mathcal{E}}_j^\dagger(z, t) \hat{\mathcal{E}}_j(z, t) | \Phi_{\text{in}} \rangle, \quad (22)$$

and their ‘‘two-photon wavefunction’’ [11, 23]

$$\Psi_{ij}(z, t; z', t') = \langle 0 | \hat{\mathcal{E}}_j(z', t') \hat{\mathcal{E}}_i(z, t) | \Phi_{\text{in}} \rangle. \quad (23)$$

The physical meaning of  $\Psi_{ij}$  is a two-photon detection amplitude, through which one can express the second-order correlation function  $G_{ij}^{(2)} = \Psi_{ij}^* \Psi_{ij}$  [11]. The knowledge of the two-photon wavefunction allows one to calculate the amplitudes  $\xi_{12}^{qq'}$  of state vector (21) via the two dimensional Fourier transform of  $\Psi_{ij}$  at  $t = t'$ :

$$\xi_{ij}^{qq'}(t) = \frac{1}{L^2} \iint dz dz' \Psi_{ij}(z, z', t) e^{-iqz} e^{-iq'z'}. \quad (24)$$

Substituting the operator solutions (20) into (22), for the expectation values of the intensities one finds

$$\langle \hat{I}_j(z, t) \rangle = |f_j(-c\tau)|^2. \quad (25)$$

For  $0 \leq z < L$  the retarded time is  $\tau = t - z/v_g$ , and therefore  $\langle \hat{I}_j(z, t) \rangle = |f_j(zc/v_g - ct)|^2$ , while outside the medium, at  $z \geq L$  and accordingly  $\tau = t - L/v_g - (z - L)/c$ , we have  $\langle \hat{I}_j(z, t) \rangle = |f_j(z + L(c/v_g - 1) - ct)|^2$ . On

the other hand, after the interaction at  $z, z' \geq L$ , the equal-time ( $t = t'$ ) two-photon wavefunction reads [27]

$$\begin{aligned} \Psi_{ij}(z, z', t) &= f_i[z + L(c/v_g - 1) - ct] \\ &\quad \times f_j[z' + L(c/v_g - 1) - ct] \\ &\quad \times \left\{ 1 + \frac{f_j[z + L(c/v_g - 1) - ct]}{f_j[z' + L(c/v_g - 1) - ct]} \right. \\ &\quad \left. \times \text{sinc} \left[ \frac{\delta q}{2} (z' - z) \right] (e^{i\phi} - 1) \right\}, \quad (26) \end{aligned}$$

where  $\phi = \eta \Delta_d L^2 \delta q / (2\pi)$ . For large enough spatial separation between the two photons, such that  $|z' - z| > \delta q^{-1}$  and therefore  $\text{sinc}[\delta q(z' - z)/2] \simeq 0$ , equation (26) yields

$$\Psi_{ij}(z, z', t) \simeq f_i[z + L(c/v_g - 1) - ct] f_j[z' + L(c/v_g - 1) - ct],$$

which indicates that no nonlinear interaction takes place between the photons, which emerge from the medium unchanged. This is due to the local character of the interaction described by the sinc function. In the opposite limit of  $|z' - z| \ll \delta q^{-1}$  and therefore  $\text{sinc}[\delta q(z' - z)/2] \simeq 1$ , for two narrow-band (Fourier limited) pulses with the duration  $T \gg |z' - z|/c$ , one has  $f_j(z)/f_j(z') \simeq 1$ , and equation (26) results in

$$\begin{aligned} \Psi_{ij}(z, z', t) &\simeq e^{i\phi} f_i[z + L(c/v_g - 1) - ct] \\ &\quad \times f_j[z' + L(c/v_g - 1) - ct]. \end{aligned}$$

Thus, after the interaction, a pair of single photons acquires conditional phase shift  $\phi$ , which can exceed  $\pi$  when  $(\delta q L / 2\pi)^2 > (v_g/c) (|\Omega_d|^2 / g^2)$ . To see this more clearly, we use equation (24) to calculate the amplitudes of the state vector  $|\Phi(t)\rangle$ :

$$\xi_{ij}^{qq'}(t) = e^{i\phi} \xi_{ij}^{qq'}(0) \exp\{i(q + q')[L(c/v_g - 1) - ct]\}. \quad (27)$$

At the exit from the medium, at time  $t \simeq L/v_g$ , the second exponent in equation (27) can be neglected for all  $q, q'$  and the state of the system is given by

$$|\Phi(L/v_g)\rangle = e^{i\phi} |\Phi_{\text{in}}\rangle. \quad (28)$$

When  $\phi = \pi$ , the output state of the two photons is

$$|\Phi_{\text{out}}\rangle = -|\Phi_{\text{in}}\rangle. \quad (29)$$

Utilizing the scheme of figure 2(b), one can then realize the transformation corresponding to the CPHASE logic gate between two photons representing qubits.

Before closing this section, we note that several important relevant issues, such as the spectral broadening of interacting pulses and the necessity for their tight focusing over considerable interaction lengths, were addressed in a number of recent studies [41, 42, 43].

## VII. SINGLE-PHOTON DETECTION

To complete the proposal for optical quantum computer, we need to discuss a measurement scheme capable of reliably detecting the polarization states of single

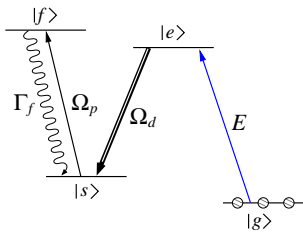


FIG. 7: Level scheme of atoms for efficient photon detection. Adiabatically switching off the driving field,  $\Omega_d \rightarrow 0$ , results in the conversion of photonic excitation  $E$  into the atomic Raman excitation  $|g\rangle \rightarrow |s\rangle$ . The latter is detected using the pump field acting on the cycling transition  $|s\rangle \leftrightarrow |f\rangle$  with Rabi frequency  $\Omega_p$  and collecting the fluorescent photons.

photons. When the photonic qubit  $|\psi\rangle = \alpha|V\rangle + \beta|H\rangle$  passes through a polarizing beam-splitter, its vertically and horizontally polarized components are sent into two different spatial modes – photonic channels. Placing efficient single-photon detectors at each channel would therefore accomplish the projective measurement of the qubits in the computational basis. The remaining question then is the practical realization of sensitive photodetectors. Avalanche photodetectors with high quantum efficiencies are possible candidates for the reliable measurement [44]. Let us, however, outline an alternative scheme [45], based on stopping of light in EIT media, whose potential efficiency is unmatched by the state-of-the-art photodetectors.

Consider an optically dense medium of four-level atoms with N-configuration of levels, as shown in figure 7. Initially, all the atoms are in the ground state  $|g\rangle$ . Under the EIT conditions discussed in section III, a single-photon pulse entering the medium can be fully stopped by adiabatically switching off the driving field Rabi frequency  $\Omega_d$ . As a result, the atomic ensemble is transferred into the symmetric state  $|s^{(1)}\rangle$  with single Raman excitation, i.e., an atom in state  $|s\rangle$ . Next, to detect the atom in this state, one can use the electron shelving or quantum jump technique [46]. To that end, one applies a strong resonant pumping laser acting on the cycling transition  $|s\rangle \leftrightarrow |f\rangle$  with Rabi frequency  $\Omega_p$  and collects the fluorescent photons emitted by the atoms with the rate  $R_f = \Gamma_f |\Omega_p|^2 / (2|\Omega_p|^2 + \gamma_{sf}^2)$ , where  $\Gamma_f$  is the spontaneous decay rate of state  $|f\rangle$ . In the limit of strong pump  $\Omega_p \gg \gamma_{sf}$ , transition  $|s\rangle \rightarrow |f\rangle$  saturates and  $R_f \sim \Gamma_f/2$ .

In alkali atoms, the cycling transition with circularly polarized pump laser can be established between the

ground and excited state sublevels  $|s\rangle = |F=2, m_F=2\rangle$  and  $|f\rangle = |F=3, m_F=3\rangle$ . To estimate the reliability of the measurement, assuming unit probability of photon trapping in EIT medium, let us suppose that a photodetector with efficiency  $\eta \ll 1$  is collecting the fluorescent signal  $S_f = \eta R_f t$  during time  $t$ . This time is limited by the lifetime of state  $|s\rangle$ ,  $\Gamma_s^{-1}$ , which is related to the Raman coherence relaxation rate by  $\gamma_R \geq \Gamma_s/2$ . A reliable measurement requires  $S_f = \frac{1}{2}\eta(\Gamma_f/\Gamma_s) \geq 1$ . Typically, in atomic vapors the ratio  $\Gamma_f/\Gamma_s \sim 10^4$ , therefore the signal  $S_f$  is very strong even for tiny efficiencies  $\eta \gtrsim 10^{-3}$ . Thus the described scheme offers great sensitivity in single- or few-photon detection.

## VIII. CONCLUSIONS

In this paper, we have described a proposal for all-optical deterministic quantum computation with photon-polarization qubits. The schemes for deterministic generation of single-photon wavepackets, their storage, manipulation, entanglement and reliable measurement were discussed. All these schemes are based on the coherent manipulation of macroscopic atomic ensembles in the regime of electromagnetically induced transparency, whose concise yet detailed description was presented for the sake of clarity and accessibility of presentation.

We have outlined the principal setup of the quantum computer and its building blocks, leaving out detailed studies of several important issues pertaining to the decoherence mechanisms and fidelity of the computer's constituent parts and their optimization, which will be addressed in subsequent publications. Certainly, the scheme described above is open to modifications and improvements, while some of its ingredients are still in the conceptual stage and have not yet been realized experimentally. It seems therefore conceivable that at least in the short term, an optimized combination of the two approaches, linear optics probabilistic [8, 34] and nonlinear deterministic discussed here, would constitute the most realistic way towards the all-optical quantum computation.

## Acknowledgments

I would like to thank M. Fleischhauer, I. Friedler, G. Kurizki, and Yu.P. Malakyan for many useful discussions and fruitful collaboration.

[1] M.A. Nielsen and I.L. Chuang, *Quantum Computation and Quantum Information* (Cambridge University Press, Cambridge, UK, 2000); D. Bouwmeester, A. Ekert, and A. Zeilinger, editors, *The Physics of Quantum Information: Quantum Cryptography, Quantum Teleportation,*

*Quantum Computation* (Springer, Berlin, 2000).

[2] A. Steane, Rep. Prog. Phys. **61**, 117 (1998); C.H. Bennett and D.P. DiVincenzo, Nature **404**, 247 (2000); A. Galindo and M.A. Martin-Delgado, Rev. Mod. Phys. **74**, 347 (2002).

- [3] D. Loss and D.P. DiVincenzo, Phys. Rev. A **57**, 120 (1998); B.E. Kane, Nature **393**, 133 (1998).
- [4] D. Petrosyan and G. Kurizki, Phys. Rev. Lett. **89**, 207902 (2002).
- [5] J.I. Cirac and P. Zoller, Phys. Rev. Lett. **74**, 4091 (1995); C.A. Sackett, D. Kielpinski, B.E. King, C. Langer, V. Meyer, C.J. Myatt, M. Rowe, Q.A. Turchette, W.M. Itano, D.J. Wineland, and C. Monroe, Nature **404**, 256 (2000).
- [6] G.K. Brennen, C.M. Caves, P.S. Jessen, and I.H. Deutsch, Phys. Rev. Lett. **82**, 1060 (1999).
- [7] Q.A. Turchette, C.J. Hood, W. Lange, H. Mabuchi, and H.J. Kimble, Phys. Rev. Lett. **75**, 4710 (1995); A. Imamoglu, H. Schmidt, G. Woods, and M. Deutsch, Phys. Rev. Lett. **79**, 1467 (1997); A. Rauschenbeutel, G. Nogues, S. Osnaghi, P. Bertet, M. Brune, J.M. Raimond, and S. Haroche, Phys. Rev. Lett. **83**, 5166 (1999).
- [8] E. Knill, R. Laflamme, and G. J. Milburn, Nature **409**, 46 (2001); J. L. O'Brien, G. J. Pryde, A. G. White, T. C. Ralph, and D. Branning, Nature **426**, 264 (2003); S. Gasparoni, J.-W. Pan, Ph. Walther, T. Rudolph, and A. Zeilinger, Phys. Rev. Lett. **93**, 020504 (2004).
- [9] R.W. Boyd, *Nonlinear Optics* (Academic Press, San Diego, CA, 1992).
- [10] S.E. Harris, Phys. Today **50**(7), 36 (1997); E. Arimondo, in *Progress in Optics*, edited by E. Wolf, (Elsevier Science, Amsterdam, 1996), vol. 35, p. 257.
- [11] M.O. Scully and M.S. Zubairy, *Quantum Optics* (Cambridge University Press, Cambridge, UK, 1997).
- [12] M.D. Lukin, M. Fleischhauer, A.S. Zibrov, H.G. Robinson, V.L. Velichansky, L. Hollberg, and M.O. Scully, Phys. Rev. Lett. **79**, 2959 (1997).
- [13] M.D. Lukin, Rev. Mod. Phys. **75**, 457 (2003).
- [14] L.V. Hau, S.E. Harris, Z. Dutton, and C.H. Behroozi, Nature (London) **397**, 594 (1999); M.M. Kash, V.A. Sautenkov, A.S. Zibrov, L. Hollberg, G.R. Welch, M.D. Lukin, Yu. Rostovtsev, E.S. Fry, and M.O. Scully, Phys. Rev. Lett. **82**, 5229 (1999); D. Budker, D.F. Kimball, S.M. Rochester, and V.V. Yashchuk, Phys. Rev. Lett. **83**, 1767 (1999).
- [15] A.B. Matsko, Yu.V. Rostovtsev, H.Z. Cummins, and M.O. Scully, Phys. Rev. Lett. **84**, 5752 (2000).
- [16] M. Fleischhauer and M.D. Lukin, Phys. Rev. Lett. **84**, 5094 (2000); Phys. Rev. A **65**, 022314 (2002).
- [17] C. Liu, Z. Dutton, C.H. Behroozi, and L.V. Hau, Nature **409**, 490 (2001); D.F. Phillips, A. Fleischhauer, A. Mair, R.L. Walsworth, and M.D. Lukin, Phys. Rev. Lett. **86**, 783 (2001).
- [18] A.V. Turukhin, V.S. Sudarshanam, M.S. Shahriar, J.A. Musser, B.S. Ham, and P.R. Hemmer, Phys. Rev. Lett. **88**, 023602 (2002).
- [19] A. Andre and M.D. Lukin, Phys. Rev. Lett. **89**, 143602 (2002); M. Bajcsy, A.S. Zibrov, M.D. Lukin, Nature **426**, 638 (2003).
- [20] H. Schmidt and A. Imamoglu, Opt. Lett. **21**, 1936 (1996).
- [21] S.E. Harris and Y. Yamamoto, Phys. Rev. Lett. **81**, 3611 (1998).
- [22] S. Harris and L. Hau, Phys. Rev. Lett. **82**, 4611 (1999).
- [23] M.D. Lukin and A. Imamoglu, Phys. Rev. Lett. **84**, 1419 (2000).
- [24] *Quantum Information with Continuous Variables*, edited by S. L. Braunstein and A. K. Pati (Kluwer Academic, Dordrecht, 2003).
- [25] H. Jeong and M. S. Kim, Phys. Rev. A **65**, 042305 (2002); T. C. Ralph, A. Gilchrist, G. J. Milburn, W. J. Munro, and S. Glancy, Phys. Rev. A **68**, 042319 (2003).
- [26] M.D. Lukin, S.F. Yelin, and M. Fleischhauer, Phys. Rev. Lett. **84**, 4232 (2000).
- [27] D. Petrosyan and Yu. P. Malakyan, Phys. Rev. A **70**, 023822 (2004).
- [28] M. Fleischhauer and C. Mewes, quant-ph/0110056; M. Fleischhauer, R. Unanyan, and C. Mewes (to be published).
- [29] *Focus on Single Photons on Demand*, edited by Ph. Grangier *et al.*, New J. Phys. **6**, (2004).
- [30] C. K. Hong and L. Mandel, Phys. Rev. Lett. **56**, 58 (1986); P. Grangier, G. Roger, and A. Aspect, Europhys. Lett. **1**, 173 (1986).
- [31] P. Michler, A. Kiraz, C. Becher, W. V. Schoenfeld, P. M. Petroff, L. Zhang, E. Hu, and A. Imamoglu, Science **290**, 2282 (2000); C. Santori, D. Fattal, J. Vukovi, G.S. Solomon, and Y. Yamamoto Nature **419**, 594 (2002).
- [32] B. Lounis and W.E. Moerner, Nature **407** 491 (2000).
- [33] M. Hennrich, T. Legero, A. Kuhn, and G. Rempe, Phys. Rev. Lett. **85**, 4872 (2000); A. Kuhn, M. Hennrich, and G. Rempe, Phys. Rev. Lett. **89**, 067901 (2002); J. McKeever, A. Boca, A.D. Boozer, R. Miller, J.R. Buck, A. Kuzmich, and H.J. Kimble, Science **303**, 1992 (2004).
- [34] L.-M. Duan, M.D. Lukin, J.I. Cirac and P. Zoller, Nature **414**, 413 (2001); A. Kuzmich, W.P. Bowen, A.D. Boozer, A. Boca, C.W. Chou, L.-M. Duan, and H.J. Kimble, Nature **423**, 731 (2003); C.H. van der Wal, M.D. Eisaman, A. Andre, R.L. Walsworth, D.F. Phillips, A.S. Zibrov, and M.D. Lukin, Science **301**, 196 (2003); C. W. Chou, S. V. Polyakov, A. Kuzmich, and H. J. Kimble, Phys. Rev. Lett. **92**, 213601 (2004); M. D. Eisaman, L. Childress, A. Andre, F. Massou, A. S. Zibrov, and M.D. Lukin, Phys. Rev. Lett. **93**, 233602 (2004).
- [35] M.D. Lukin, M. Fleischhauer, R. Cote, L.M. Duan, D. Jaksch, J.I. Cirac, and P. Zoller, Phys. Rev. Lett. **87**, 037901 (2001).
- [36] T.F. Gallagher, *Rydberg Atoms* (Cambridge University Press, Cambridge, 1994).
- [37] M. Saffman and T. G. Walker, Phys. Rev. A **66**, 065403 (2002).
- [38] D. Petrosyan and G. Kurizki, Phys. Rev. A **65**, 033833 (2002).
- [39] C. Ottaviani, D. Vitali, M. Artoni, F. Cataliotti, and P. Tombesi, Phys. Rev. Lett. **90**, 197902 (2003).
- [40] S. Rebic, D. Vitali, C. Ottaviani, P. Tombesi, M. Artoni, F. Cataliotti, and R. Corbalan, Phys. Rev. A **70**, 032317 (2004).
- [41] I. Friedler, G. Kurizki and D. Petrosyan, Europhys. Lett. **68**, 625 (2004); Phys. Rev. A **71**, xxx (2005).
- [42] M. Masalas and M. Fleischhauer, Phys. Rev. A **69**, 061801(R) (2004).
- [43] I. Friedler, G. Kurizki, D. Petrosyan and M. Fleischhauer (to be published).
- [44] P.G. Kwiat, A.M. Steinberg, R.Y. Chiao, P.H. Eberhard, and M.D. Petroff, Phys. Rev. A **48**, R867 (1993); S. Takeuchi, J. Kim, Y. Yamamoto, and H. Hogue, Appl. Phys. Lett. **74**, 1063 (1999).
- [45] A. Imamoglu, Phys. Rev. Lett. **89**, 163602 (2002); D.F.V. James and P.G. Kwiat, Phys. Rev. Lett. **89**, 183601 (2002).
- [46] W. Nagourney, J. Sandberg, and H. Dehmelt, Phys. Rev. Lett. **56**, 2797 (1986); T. Sauter, W. Neuhauser, R. Blatt, and P.E. Toschek, Phys. Rev. Lett. **57**,

1696 (1986); J.C. Bergquist, R.G. Hulet, W.M. Itano, and D.J. Wineland, Phys. Rev. Lett. **57**, 1699 (1986); M.B. Plenio and P.L. Knight, Rev. Mod. Phys. **70**, 101 (1998).